Vol. 585: 31–48, 2017
https://doi.org/10.3354/meps12370

MARINE ECOLOGY PROGRESS SERIES
Mar Ecol Prog Ser

Published December 27

Mapping the diversity of spectral shapes discriminates between adjacent benthic biophonies

J. Lossent[1,2,3,*], L. Di Iorio[1,3,4], C. A. Valentini-Poirier[5], P. Boissery[5], C. Gervaise[1,4]

[1]Research Institute CHORUS, 38000 Grenoble, France
[2]France Energies Marines, 29200 Brest, France
[3]Gipsa-lab, CNRS & Grenoble INP, UMR 5216, 38402 Grenoble, France
[4]Chair Chorus, Foundation of Grenoble Institute of Technology, 38000, Grenoble, France
[5]French Water Agency Rhône Méditerranée Corse (RMC), 13001 Marseille, France

ABSTRACT: Coastal soundscapes are dominated by broadband transient sounds primarily emitted by benthic invertebrates. These sounds are characterized by a very large dynamic of amplitude. The loudest ones propagate further and interfere with the detectability of benthic sounds by invading other more distant habitats. Acoustic diversity assessment is therefore biased when applying acoustic indices related to the signal's power. Here, we propose new acoustic indices (IDSS: indices of the diversity of spectral shape) capable of extracting the diversity of the benthic invertebrate biophony (BIB) despite interference from loud and abundant sounds. A passive acoustic ecological survey was conducted in a shallow Mediterranean bay with a small-scale mosaic of biocenosis. The sound pressure level and spectrum of the BIB revealed that the rocky fringe had the most powerful biophony, propagating up to 3680 m, thus 'invading' other habitats. However, these power-based indices failed to depict BIB diversity. The IDSS allowed us to discriminate BIB diversity despite the interfering rocky fringe biophony, including low-power sounds not depicted by traditional power-based methods. Four main categories of benthic invertebrates sounds (BIS) spectra were found. Two categories (high-power, peak frequencies ~3 to 4 kHz) were mainly linked to the rocky fringe. Their contribution to the diversity (56%) decreased with increasing distance to the fringe, where low-power BIS (peak frequencies above 15 kHz) predominantly contributed to the BIB (42%) and may be specific to coralligenous reefs. The IDSS enables a better characterization and quantification of BIB diversity and soundscape structure with a fine spatial resolution (~200 m).

KEY WORDS: Soundscape ecology · Mapping biophony · Passive acoustic ecological survey · Benthic invertebrate sounds · Acoustics indices · Diversity of spectral shapes · Acoustic monitoring

INTRODUCTION

The underwater soundscape is a collection of sounds that emanates from a marine landscapes or passes through it (Krause 1987). It is composed of natural abiotic ambient sounds (geophony; Kinda et al. 2013, 2015, Mathias et al. 2016), anthropogenic sounds (anthrophony; Hildebrand 2009, Gervaise et al. 2012) and sounds from marine fauna (biophony). The main contributors to biophony are cetaceans (Au & Hastings 2008), fishes (Amorim 2006, Rountree et al. 2006, Luczkovich et al. 2008) and benthic invertebrates (Patek 2001, Popper et al. 2001, Coquereau et al. 2016a). Benthic invertebrates emit a variety of isolated transient sounds that eventually create mass phenomena such as choruses. Snapping shrimps (among the Alpheidae family) produce among the loudest sounds in marine coastal environments, and are known to dominate the soundscapes of coastal environments (Johnson et al. 1947, Au & Banks 1998,

*Corresponding author: julie.lossent@chorusacoustics.com

Versluis et al. 2000, Chitre et al. 2012). However, the benthic invertebrate biophony goes beyond the contribution of snapping shrimps, since sea urchins (Radford et al. 2008), crustaceans (Popper et al. 2001, Coquereau et al. 2016b), bivalves (Di Iorio et al. 2012) and benthic populations in general (Coquereau et al. 2016a) are also known to produce audible and distinct acoustic signals (namely broadband transient signals) while feeding, moving, etc. Altogether, these sounds, in this study referred to as benthic invertebrate sounds (BIS), contribute to benthic invertebrate biophony (BIB).

During the last decade, it has been shown that underwater soundscapes are used by larvae of vertebrate and invertebrate marine organisms as a cue to choose a suitable habitat for their development during the transition from the pelagic to the coastal phase (Montgomery et al. 2006, Stanley et al. 2012, Parmentier et al. 2015, Lillis et al. 2015), and then used by adults to move towards feeding and breeding areas (Ellers 1995, Simpson et al. 2005, Huijbers et al. 2012). This new field of study (referred to as ecoacoustics, Sueur & Farina 2015; or soundscape ecology, Pijanowski et al. 2011) mirrors marine fauna use of soundscape features, to infer information on biodiversity and to assess populations (Sueur et al. 2008, 2014, Zenil et al. 2011, Nedelec et al. 2015, Hastings & Širović 2015, Harris et al. 2016), ecological process (Hawkins 1986, Crawford et al. 1997, Acevedo-Gutiérrez & Stienessen 2004, Amorim 2006, Radford et al. 2008, Di Iorio et al. 2012, Coquereau et al. 2016a), to link soundscape features to oceanographic processes or properties of the habitat or the environment (Mann & Grothues 2009, McWilliam & Hawkins 2013, Nedelec et al. 2015, Ruppé et al. 2015) as well as to infer their state of conservation/degradation (Watanabe et al. 2002, Piercy et al. 2014, Harris et al. 2016, Coquereau et al. 2016c, 2017). To carry out these passive acoustic ecological surveys (PAES) (McWilliam & Hawkins 2013), underwater soundscapes are studied on ecologically relevant time periods and on several sites with contrasting biodiversity, habitats and environmental quality properties. Acoustic measurements are described through the prism of one or more indices. Table S1 in the Supplement at www.int-res.com/articles/suppl/m585p031_supp.pdf summarizes the studies dealing with acoustic spatial variability that were carried out between 2010 and 2016 to our knowledge, ordered according to the spatial scale studied.

For the references outlined in Table S1, the existence of significant statistical dependencies between acoustic indices and environmental parameters unambiguously demonstrates the relevance of PAES. However, with the exception of McWilliam & Hawkins (2013), these recent studies realize a proof-of-concept by choosing either sufficiently large spatial scales so that the sampling points are acoustically isolated from each other (i.e. the soundscapes recorded at each measurement point do not overlap) or very different, contrasting habitats. The indices used are mainly based on the acoustic power in a given frequency band (sound pressure level [SPL] in dB re 1 µPa), on the acoustic power as a function of the frequencies (power spectrum) and on the number of powerful biological sounds (BIS counts) (Table S1). These power-based indices are appropriate in the context of larval, juvenile and adult recruitment, where we suppose that the suitable habitats for larval development have a specific and louder acoustic signature.

The marine environment facilitates the propagation of acoustic waves (Urick 1967), and noise levels emitted by different sound sources such as bivalves, echinoderms or crustaceans can be very different (Ferguson & Cleary 2001, Coquereau et al. 2016a). Describing a biophony at a sampling point based on its power or number of BIS per unit of time can mask low-power but ecologically relevant pulses. Consequently, this masking could significantly skew the results of PAES aimed at assessing the biodiversity of a site, as only high-energy BIS (such as those produced by snapping shrimps) are taken into account. This effect is very well illustrated and explained by McWilliam & Hawkins (2013), who studied the soundscape of a small bay (600 × 400 m) with a patchwork of 4 habitats. They showed that the variability of the acoustic indices was more related to the distance between the measurement points and the site hosting snapping shrimps than to the nature of the habitat at the sampling point itself.

Working with indices of acoustic power also raises the question of spatial resolution in the acoustic characterization of a site. We suggest defining it as the propagation distance of the most powerful biological sound source in the environment studied. For example, if it is the snapping shrimp, then the propagation radius may be >3000 m (source level taken from Ferguson & Cleary 2001; propagation distances calculated as described in Coquereau et al. 2016a). In this propagation area (3 km), it would be impossible to distinguish the acoustic presence of feeding sea urchins *Echinus* spp. (propagation distance 12 m; Coquereau et al. 2016a) or decapod crustaceans *Maja brachydactyla* (feeding activity, propagation distance 42 m; Coquereau et al. 2016a) for instance. These simple 'theoretical' considerations are con-

firmed by *in situ* measurements. Lillis et al. (2014b) suggest that the propagation distance of the biophony of an oyster reef set on a soft bottom is >500 m for a sea state <3 on the Beaufort scale. Piercy et al. (2014) and Radford et al. (2011) describe propagation distances >1500 m for coral and rocky reefs.

However, to be an efficient tool for ecological diagnosis, PAES should have a spatial resolution adapted to that of benthic communities between and within habitats. The spatial variability of benthic communities in coastal habitats is significant at small scales, beyond 1 km. This has been shown for the type of habitats investigated in the studies presented in Table S1, including hard-bottom substrates (Archambault & Bourget 1999, Terlizzi et al. 2007), rocky and coral reefs (Anderson & Millar 2004) and seagrass (Bell & Westoby 1986).

The aims of the present study were to (1) test the hypothesis that loud benthic sound sources such as snapping shrimps 'invade' the soundscape of other habitats and mask sounds from other organisms and (2) propose new acoustic indices that assess and quantify the indices of diversity of the spectral shapes (IDSS) and are capable of revealing the presence of transient sounds with low amplitudes that are potentially masked by loud sound sources if only power-based descriptors were used (SPL, power spectrum). By doing this, we aimed at improving the spatial resolution of PAES below the sub-km (~200 m) and thus to an ecologically relevant scale.

MATERIALS AND METHODS

Study site

The study site was the bay of la Revellata, Calvi, Corsica, France (42° 34′ 49″ N, 8° 43′ 27″ E). Data collection occurred from 3 to 9 August 2014 at the oceanographic station STARESO thanks to its program STARECAPMED (Richir et al. 2014). The bay of la Revellata (~4 km^2) hosts a mosaic of 4 habitats including subtidal rocky reef, seagrass, sand and massive coralligenous reefs (Fig. 1). Water depth ranges

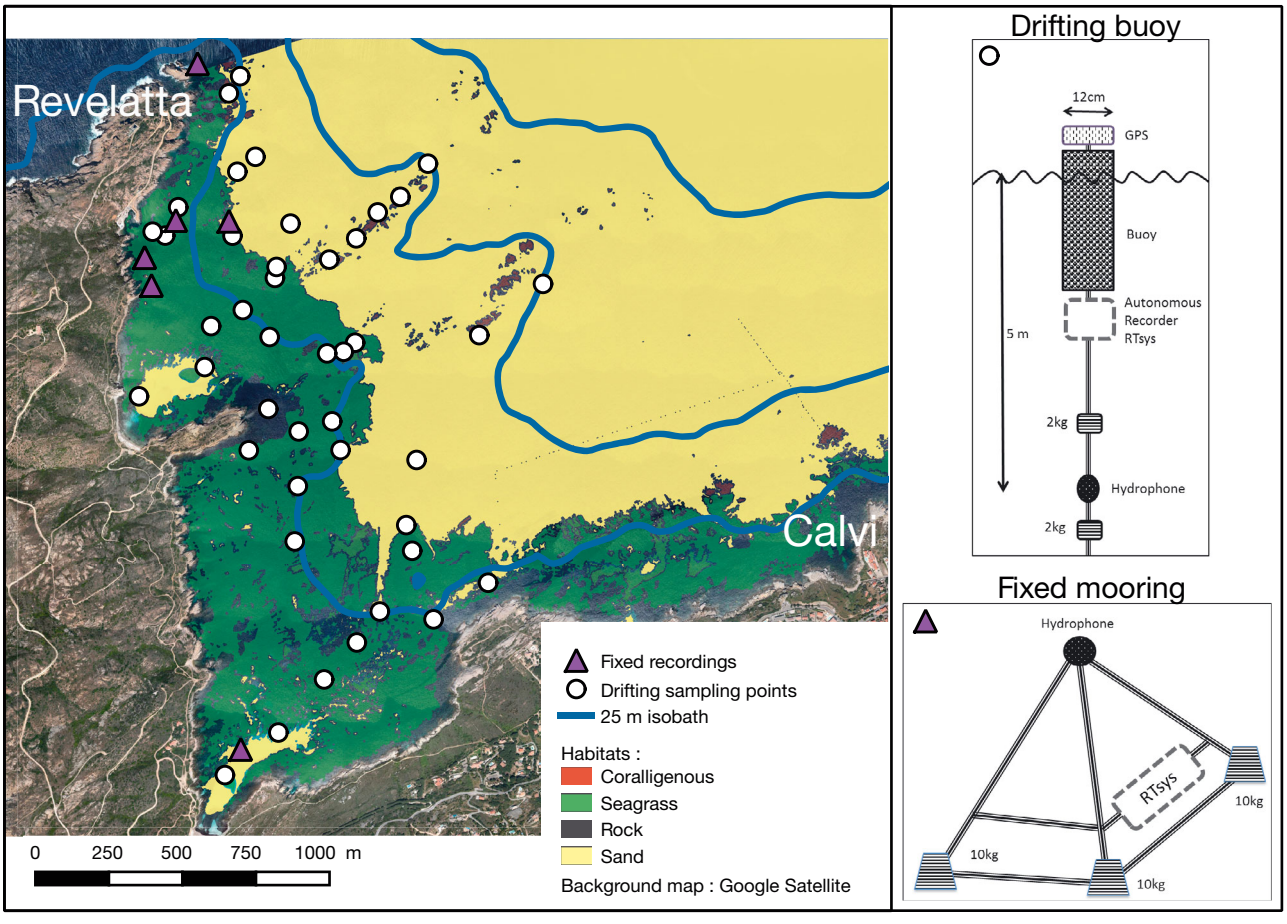

Fig. 1. Bay of la Revellata showing habitat layers and deployment site with drifting sampling points (white circles) and fixed recording points (purple triangles) (QGIS Development Team 2009)

from 0 to 50 m. Subtidal rocky reefs constitute 0.307 km^2 (7.6% of the study area) and are confined to the 7.2 km coastline. This rocky fringe produces a very powerful biophony mainly consisting of snapping shrimp sounds. Seagrass *Posidonia oceanica* covers 1.525 km^2 (40% of the study area). It is present between 8 and about 37 m depth and stretches over a distance of 5 km at a width varying from 45 m to 1 km. The seagrass is well preserved in comparison to other places in the Mediterranean sea (Gobert et al. 2009, Lejeune et al. 2013, Holon et al. 2015), with the exception of a small area degraded by boat anchors moored in the bay during the summer months (Lejeune et al. 2013, Richir et al. 2014). Beyond a depth of 37 m, sand is the major habitat in terms of surface coverage (49.4% of the study area). Several massive coralligenous reefs emerge from the sandy habitat, comprising only 43 900 m^2 (1.1% of the overall study area). The site is described as 'in good ecological state' and hosts a rich biodiversity (Seytre & Francour 2009, Gobert et al. 2014).

Acoustic recordings

PAES was performed using a drifting buoy and 2 fixed bottom moorings. The drifting buoy captured the spatial variability with short recordings in several positions, while the fixed mooring allowed us to estimate the source levels of the BIB emitted and validate the propagation model given by the drifting recording positions. The drifting buoy and fixed moorings were equipped with an autonomous recorder SDA 14 (RTSYS®) and a HTI-92-WB (High Tech Inc.®) hydrophone with a flat sensitivity equal to −155 ± 3 dB re 1 V μPa^{-1} between 5 and 50 kHz. Acoustic recordings were sampled at a rate of 156 kHz at a 24-bit resolution. The hydrophone was located 5 m below the sea surface on the drifting buoy and 1 m above the sea bottom on the fixed moorings (Fig. 1). The drifting buoy was deployed at 44 predefined positions from a 5 m long boat. After deployment, the boat moved 100 m away and stopped the engine in order to avoid noise interference. After 20 min of recording, the buoy was recovered. At each deployment and recovery, GPS time and position were noted. Daytime drifts were conducted on 5, 6, 7 and 9 August between 08:00 and 18:00 h. A total of 14, 10, 8 and 12 drifts were carried out respectively. The fixed hydrophones were deployed on 3, 4 and 8 August. Because of logistic constraints, fixed and drifting recordings could not be carried out on the same days. The fixed mooring was deployed and recovered by divers at 6 predefined positions for continuous 24 h recordings (Table 1). Because water depths exceed 30 m at the coralligenous reef sites, fixed recordings could not be carried out due to the limited license of the diver team. During the entire campaign, winds were limited and stable (3 ± 1.9 m s^{-1}), mean surface temperature was 24.2 ± 0.4°C and the temperature profile had a thermocline at 50 m with a corresponding temperature of 15 ± 0.1°C.

Data processing

Data selection and grouping

The recordings were divided into 10 s snapshots. For each snapshot, a spectrogram was calculated (Hanning window, 50% overlap, 2048 Pt. fast Fourier transform [FFT]) comprising 1524 spectra. The spectrograms were visually inspected and snapshots containing boat noise were rejected. Only daytime recordings (8:00 to 19:00 h) were used for the analyses. An overview of the samples we used is presented

Table 1. Summary of the measurement points, their relative partitioning by habitat and samples used for data analysis. A snapshot is a portion of 10 s recordings; each snapshot contains 1524 spectra of 6.56 µs. Only snapshots that could be used for the analysis (without boat noise), are considered in this table

	Habitat	No. of measurement points	Mean distance to coast (m)	No. of 10 s snapshots	No. of spectra selected for analysis Per habitat	Total
Drifting buoy	Rock	5	99.3	110	167640	873252
	Seagrass	28	251.4	345	525780	
	Sand	6	885.3	68	103632	
	Coralligenous	5	766	50	76200	
Fixed mooring	Rock	2	35	450	685292	2055876
	Seagrass	3	250	786	1199261	
	Sand	1	400	112	171323	
	Coralligenous	0	–	0	0	

in Table 1. A total of 1921 snapshots of 10 s, corresponding to 2 929 128 spectra were selected. Overall, 58% of the measurements were made on seagrass, 29% on rocky habitats, 9% on sand and 2% on coralligenous reefs (Table 1). Given the findings of previous work (see Table S1 in the Supplement), we tested the hypothesis that the powerful biophony (i.e. snapping shrimps) emanating from subtidal rocky reef invades and dominates other, more distant habitats. For each measurement position (drifting or fixed recording), we measured the distance between the sampling point and the nearest point on the coastline. This distance varied between 62 and 1934 m. Since the rocky reef is concentrated along the coastline, the distance to the coastline is a reliable approximation of the distance to the nearest rocky habitat (i.e. snapping shrimp). We grouped the data into 4 quartiles of distance 'r' between the measurement positions and the coastline (Q1: 0 m ≤ r < 157 m; Q2: 157 m ≤ r < 293 m; Q3: 293 m ≤ r < 514 m; Q4: r ≥ 514 m) (see Table S2 in the Supplement). The quartiles were separated this way in order to have as many measurement points as possible in each quartile (11 of 44). The 4 quartiles were acoustically sampled each day.

For data analysis, we used several partitioning scales (Tables 1 & S2, Fig. 2): the snapshot, the measurement point (multiple snapshots), the quartile or region (Q1 to Q4; several measurement points) and the whole database (several regions). Working at the snapshot scale allowed us to assess the variability of acoustic descriptors at higher partitioning levels (e.g. area) and to compute bootstrap analyses.

Data analysis consisted of the evaluation of 3 acoustic descriptors: SPL (dB re 1 µPa) of the impulsive broadband BIS (SPL_{Imp}) in the band [1.5–40 kHz], and the power spectrum (dB re 1 µPa^2 Hz^{-1}) in the band [1.5–40 kHz], (which represent the descriptors classically used by the community), and a new descriptor depicting and quantifying the diversity of spectral shapes of a snapshot of data based on principal component analysis (PCA), after normalizing for the power component.

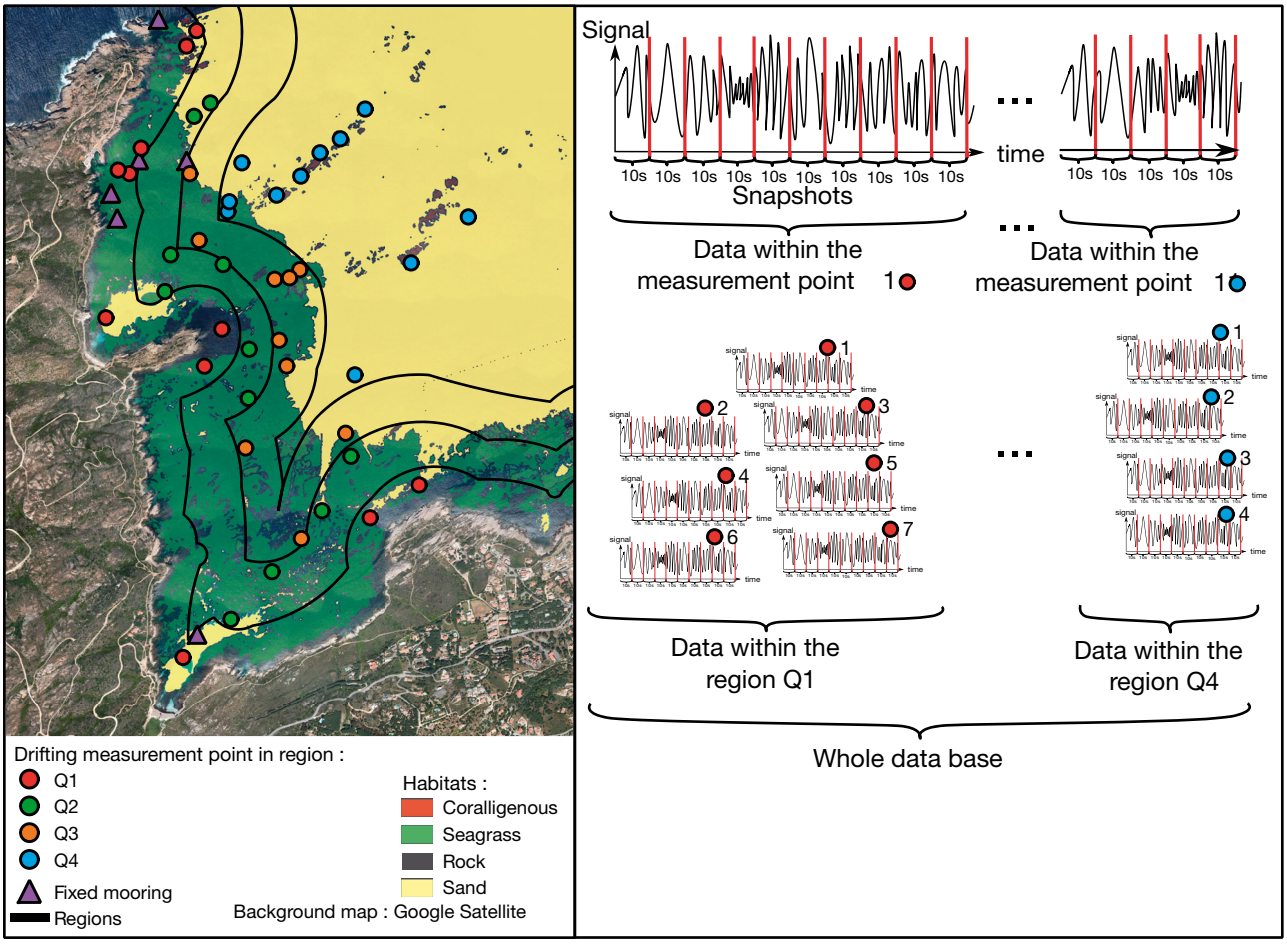

Fig. 2. Schematic representation of the different partitioning levels of the acoustic data, by region (each quartile [Q1–Q4] includes 11 drifting sample-points; in Q3, 2 sample-points overlap)

SPL_{Imp} of BIS [1.5–40 kHz] (dB re 1 µPa) used as relevant acoustic indices

After examination of the spectrograms (see Fig. 3) and percentile of the spectra (see Fig. 5), we selected the biological frequency band of [1.5–40 kHz], called 'B_b' (consistent with those used in previous works; cf. Table S1). Over the duration of the 2048 sample FFT windows, i.e. 13 ms, we computed a spectrogram and calculated the broadband SPL by integrating over the acoustic spectrum (dB re 1 µPa^2 Hz^{-1}) in the band B_b. The SPL (dB re 1 µPa) calculated here reflects the root mean square (RMS). Each 10 s snapshot provides 1524 SPL (RMS) values. We used the 95th percentile of these values as an indication of the power of the BIS (SPL_{Imp}).

To study the 'invasive' nature of powerful BIS emitted from the rocky reef over other adjacent habitat types, we estimated the propagation distance of its biophony. We fitted a logarithmic regression law to the data using a linear least square minimization of SPL_{Imp} with $\log_{10}(r)$ assuming the following model:

$$SPL_{Imp}(r) = SPL_1 + k \times \log_{10}(r) \quad (1)$$

where r is the distance to the rocky reef, SPL_1 (dB re 1 µPa at 1 m) is the noise level emitted at 1 m from the coast and $k \times \log_{10}(r)$ represents transmission losses (TL) at a distance of r m.

To estimate propagation distances of this biophony, we calculated the ambient noise level assuming a given wind speed by integrating Wenz's empirical spectrum (Wenz 1962) over B_b. We then found the distance, r, for which $SPL_{Imp}(r)$ was equal to the ambient noise level.

Spectrum-based acoustic indices dB re 1 µPa^2 Hz^{-1} in [1.5–40 kHz]

For this analysis, we used the spectra $\gamma(f)$ dB re 1 µPa^2 Hz^{-1} of the drifting recordings calculated with length of the FFT equal to 2048. For each snapshot of 10 s comprising 1524 spectra, we selected the spectra belonging to BIS (i.e. forming the 95th percentile or more, namely 76 spectra snapshot^{-1}). We worked at the scale of regions Q1, Q2, Q3 and Q4 (Fig. 2) by combining all selected spectra recorded on Q1, Q2, Q3 or Q4. For each frequency, we evaluated the mean and standard deviation of the spectra from a given region.

Then for each spectrum, we extracted 2 spectral indices. The first is the mean power spectrum over B_b:

$$D1 : \gamma_{imp}(f) \quad (\text{dB re } 1\ \mu\text{Pa}^2\ \text{Hz}^{-1}),\ f \in [1.5\text{–}40\ \text{kHz}] \quad (2)$$

The second characterizes the shape of the spectral peaks due to the biophony independent of their amplitude:

$$D2 : \gamma_{norm}(f) = \frac{(\gamma_{imp}(f) - \gamma_0)}{\sigma_\gamma}, \quad f \in [1.5 - 40\text{kHz}]$$
$$\text{with } \gamma_0 = \frac{1}{B_b}\int_{1.5\text{kHz}}^{40\text{kHz}} \gamma_{imp}(f)\,df \quad (3)$$
$$\text{and } \sigma_\gamma = \sqrt{\frac{1}{B_b}\int_{1.5\text{kHz}}^{40\text{kHz}} (\gamma_{imp}(f) - \gamma_0)^2\,df}$$

with $\gamma_{norm}(f)$ expressed in arbitrary units.

For frequencies of B_b, spectra were tested for normal distribution (1-sample Kolmogorov-Smirnov test, $H = 0$, $p > 0.5$) and homogeneity of variances of the 4 regions (Q1, Q2, Q3, Q4). We found a maximum relative error of 32 % between the lowest standard deviation compared to the highest one of the descriptor $D1$ evaluated for each region, and 66 % between the standard deviations of the descriptor $D2$ evaluated for each region. To test whether mean power spectral density (descriptor $D1$) and spectral shape (descriptor $D2$) from different regions shared the same mean, we applied an ANOVA for each frequency bin (given by the FFT window size) as described in Bertucci et al. (2015) but using the bootstrapping method (Efron & Tibshirani 1985). We randomly selected 100 values of $D1$ and $D2$ for each region and tested whether the descriptors shared the same means between {Q1, Q2, Q3, Q4}, {Q1, Q2}, {Q1, Q3} and between {Q1, Q4}. We repeated this operation 200 times. Although not strictly equal, the standard deviation of $D1$, $D2$ are of the same order across the regions Q1, Q2, Q3 and Q4, and ANOVA is known to be robust to deviations of the assumption of a strict homogeneity of variance for equal group sizes, which is the case for our bootstrapping method (Glass et al. 1972).

IDSS based on PCA as relevant acoustics indices

To determine the IDSS (indices of the diversity of the spectral shapes), We used the spectra $\gamma(f)$ dB re 1 µPa^2 Hz^{-1} as described in the above section. Because transient benthic sounds have a poor frequency resolution (Coquereau et al. 2016a) and to reduce the dimensions for the PCA, each spectrum was subsampled on 64 uniformly distributed frequency bins in the biological frequency band B_b after a smoothing by a moving average of γ(f) on a 2 kHz bandwidth.

For each snapshot of 10 s, consisting of 1524 spectra, we selected the spectra belonging to BIS (i.e. forming the 95th percentile or more, namely 76 spectra per snapshot).

First, these spectra were adjusted to have a normalized energy unit:

$$\gamma_u(f) = \frac{\gamma_{\mathrm{imp}}(f)}{\int_{1.5\mathrm{kHz}}^{40\mathrm{kHz}} \gamma(u)\,du} \quad f \in [1.5-40\ \mathrm{kHz}] \text{ and } u \in [1.5-40\ \mathrm{kHz}] \tag{4}$$

This correction eliminates the notion of amplitude of the spectrum but retains its shape.

We conducted a PCA on all spectra of BIS. PCA identified a basis of 64 orthonormal vectors and each initial spectrum was then characterized by 64 scores α_i (i from 1 to 64) as the coordinates of the spectrum on the orthonormal basis of the PCA. The linear combination of the first 2 components of the PCA defines a smoothed approximation of the true spectra. This approximation is fully described by the 2 scores (α_1, α_2). For the entire drifting dataset (873 252 spectra), we computed the occurrence probability density function of the scores (α_1, α_2). We characterized the spectral shape through the signs (positive or negative) of the first 2 coordinates (α_1, α_2). The spectral shapes were separated into 4 categories prima facie arbitrarily (cf. 'Discussion' for a more detailed explanation about this choice) according to their positions in the plane (α_1, α_2). A spectrum with the scores (α_1, α_2) belongs to the category 'Shape 1' (S1) if $\alpha_1 > 0$ and $\alpha_2 > 0$, to 'Shape 2' (S2) if $\alpha_1 > 0$ and $\alpha_2 < 0$, to 'Shape 3' (S3) if $\alpha_1 < 0$ and $\alpha_2 < 0$ and to 'Shape 4' (S4) if $\alpha_1 < 0$ and $\alpha_2 > 0$.

For a segment of data and its set of spectra, we suggest describing the diversity of spectral shapes of the BIS by expressing the proportions P1, P2, P3 and P4 of the pulses belonging to the families S1, S2, S3 and S4 respectively. This can be done at different partitioning levels according to the scope of the analysis (the snapshot, measurement point, region; Fig. 2) and allows quantifying spectral diversity at any given level. The quadruplet of proportions {P1, P2, P3, P4} is the new descriptor of the diversity of the spectra shapes (IDSS).

For statistical analysis of the IDSS, we first checked the normal distribution of the proportions P1, P2, P3 and P4 (1-sample Kolmogorov-Smirnov test, $H = 0$, $p > 0.7$) and the uniformity of their variances (maximum relative error of 22% between the lowest standard deviation compared to the highest). To test if the regions Q1, Q2, Q3 and Q4 shared the same proportions of spectral shapes, we conducted a bootstrap MANOVA using the vector of proportions {P1, P2, P3, P4} of each 10 s snapshot between the regions. Since at least 1 of the 4 proportions is linearly related to the other 3 by P1 + P2 + P3 + P4 = 1, we only considered 3 of the 4 proportions together {P1, P2, P3} for this analysis. Because different spectral shapes likely correspond to different benthic assemblages, we performed bootstrap ANOVAs for each of the 4 proportions to assess whether the regions shared the same mean values of P1, P2, P3, P4 taken separately. Bootstrap ANOVA and MANOVA were conducted using 1000 times 50 randomly chosen snapshots by region.

RESULTS

Overview of the data with typical spectrograms

Fig. 3 presents typical spectrograms of measurements from different habitats as well as from anthropogenic noises omitted from any analyses. The 2 spectrograms illustrating noise due to boats show very specific records that are used to unambiguously reject the polluted data. The habitat-related spectrograms clearly show the powerful vertical lines between 1.5 and 40 kHz representing the transient sounds produced by benthic invertebrates.

Data analysis with SPL_{Imp} [1.5–40 kHz] as relevant acoustics indices

The SPL_{Imp} (dB re 1 µPa) significantly decreased as a function of distance r ($R^2 = 0.55$, $p < 0.001$) (Fig. 4). The best linear regression, explaining 55% of the variance was expressed by:

$$SPL_{Imp}(r) = 147 - 14\log_{10}(r) \tag{5}$$

The regression model fits to the SPL_{Imp} measurements. This is compatible with the hypothesis of a strong sound source present on coastal rocky reefs that propagates offshore. The value SPL_1 (147 dB re 1 µPa at 1 m) quantifies the source level of the biophony of the rocky reef, and k (14 dB decade^{-1}) quantifies the transmission losses. The propagation distance of the benthic biophony of the rocky reef is 3680 m at a wind speed of 3 m s^{-1} (mean wind speed during the PAES Revellata-2014 campaign), 1371 m for 6 m s^{-1} wind speed and 511 m for 12 m s^{-1} wind speed. Fixed and drifting measurements both produced data in agreement with the regression. This implies that despite the difference in the distance between the sensor and the seafloor, the 2 recording systems show equivalent sound level values.

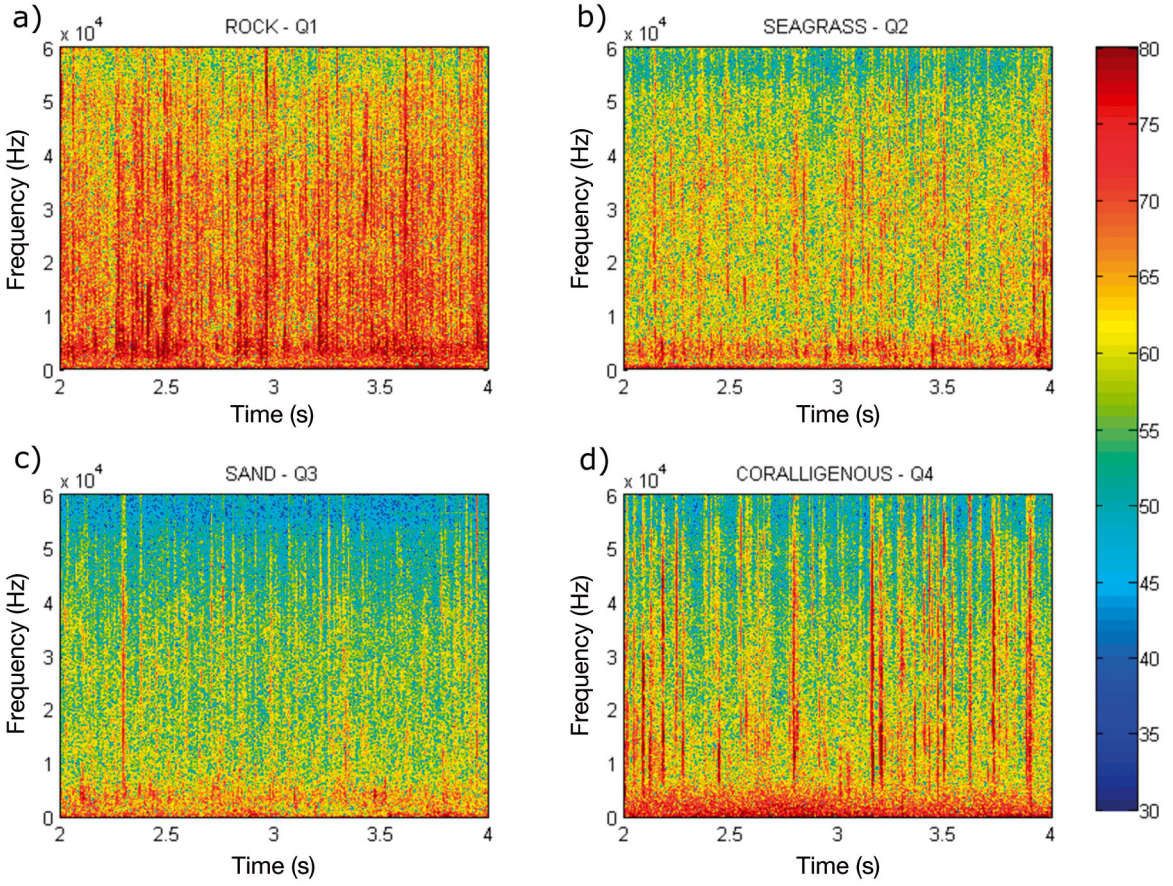

Fig. 3. Typical spectrograms showing visual representations of the spectrum of frequencies of sound, with the time on the *x*-axis and frequencies on the *y*-axis. (a) Rocky reef in region Q1; (b) seagrass in region Q2; (c) sandy habitat in region Q3; and (d) coralligenous reefs in region Q4. Scale bar: dB re 1 µPa^2 Hz^{-1}

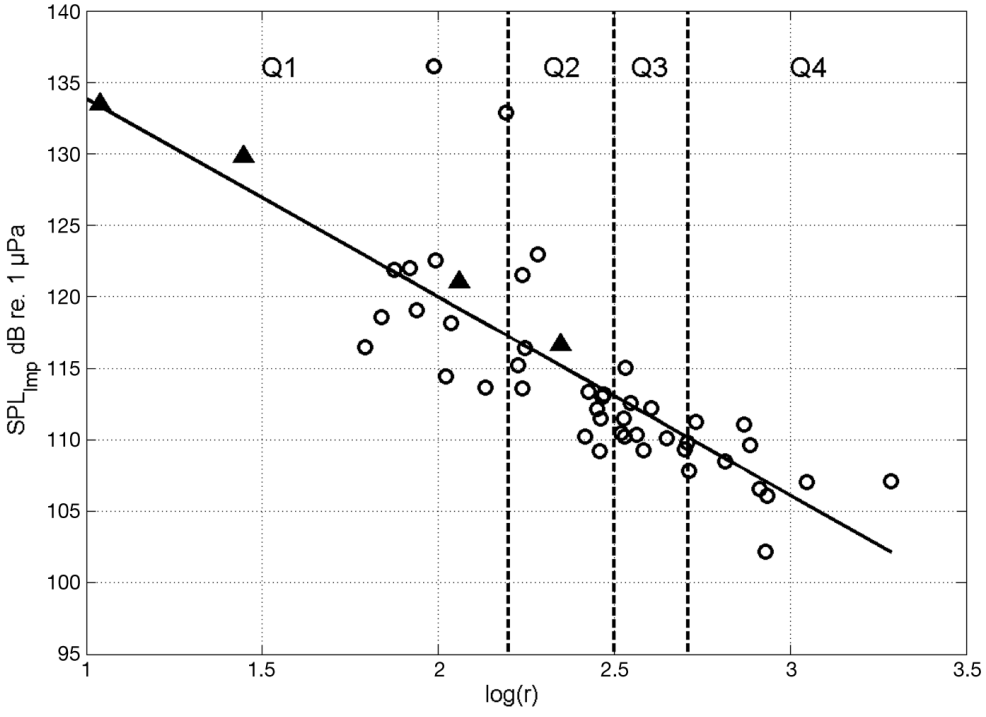

Fig. 4. Sound pressure level of impulsive broadband sounds (SPL_{Imp}) as a function of distance *r* (in meters) from the coastline. Triangles: fixed measurement points; circles: drifting buoys on rocky reef, seagrass, sand and coralligenous reefs; solid line: best fit; dashed line: limit of region Q1 ($r < 158$ m), Q2 (158 m < $r < 316$ m), Q3 (316 m < $r <$ 514 m) and Q4 ($r > 514$ m)

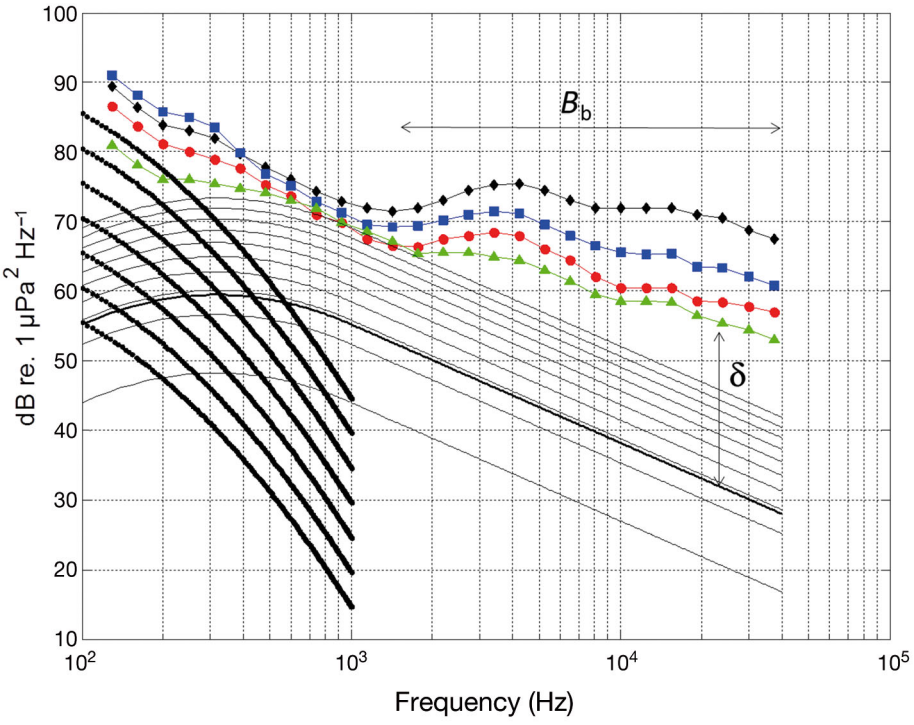

Fig. 5. Mean of the spectra from regions Q1 (black diamonds), Q2 (blue squares), Q3 (red circles) and Q4 (green triangles) superposed on the empirical Wenz spectra (Wenz 1962). Thick black curves: shipping noise spectra for index 1 to 7; thin black curves: noise due to wind for wind speed 0 to 15 m s^{-1}; medium black curve: Wenz spectra for a wind speed equal to the median of the wind speeds during the PAES Revellata-2014 field work (3 ± 1.9 m s^{-1}). B_b: bethic frequency band [1.5 kHz–40 kHz]; δ: deviation of measured spectra from windspeed median

Data analysis with spectrum-based acoustics indices $\gamma_{Imp}(f)$ [1.5 kHz < f < 40 kHz]

Mean spectra of the regions Q1, Q2, Q3 and Q4 correspond to the upper limit of Wenz's model for frequencies below 1000 Hz (Fig. 5). We believe this large level is not created by shipping in the bay of la Revellata, but rather by the sound of breaking waves (nearshore surf noise) and the chorus of several fish species (Buscaino et al. 2016). Beyond 1500 Hz, the spectra deviate positively from Wenz's model by at least 20 dB with respect to the average wind regime during data collection (δ in Fig. 5).

The region corresponding to the quartile of the data recorded near rocky reef, Q1, produced the loudest biophony compared to the other regions (5.3 ± 1.7 dB more than Q2, 9.2 ± 2.5 dB more than Q3 and 11.7 ± 2.8 dB more than Q4 (Fig. 6a). Mean spectral shapes for the regions Q1, Q2, Q3 and Q4 are very similar (Fig. 6b). Standard deviation spectra varied little with frequency in the band B_b.

Descriptor $D1$ showed significant differences for all frequencies tested (ANOVA, $p < 0.05$, $F = 41$, df = 19; Fig. S1 in the Supplement). In the case of descriptor $D2$, for frequencies greater than 2000 Hz, the normalized spectra share the same average shape (ANOVA, $p > 0.65$, $F = 0.14$, df = 19; Fig. S1).

Data analysis with IDSS

The first 2 eigenvalues of the PCA capture 55% of the total variance of the spectra. The first component explains 33% of the variance and the second one explains 22%. Beyond this, each additional eigenvalue explains very little variance: an additional 3% is provided by the 3rd eigenvalue, explaining 58% of the total variance; 42 of the 64 eigenvalues are necessary to capture 98% of the variance of the normalized spectra (see Fig. S2 in the Supplement).

Fig. 7a shows the density of probability of the scores (α_1, α_2) for all the BIS spectra. Overall, 12% (P1) of the BIS belong to the category S1, 29% of the BIS (P2) belong to S2, 33% of the BIS (P3) belong to S3 and 26% of the BIS (P4) belong to S4. Category S1 (cf. Fig. 7b) contains high energetic spectra with a marked maximum at 3 kHz and a bandwidth of about 2 kHz. Category S2 (cf. Fig. 7b) contains high energetic spectra with a marked maximum at 4 kHz, with a bandwidth of about 2 kHz and a slight rise at 10 kHz. These 2 categories have similar characteristics, and together represent 41% of all spectra. Category S3 (cf. Fig. 7b) contains mid-amplitude spectra and a wide frequency band between 3 and 15 kHz. Category S4 (cf. Fig. 7b) contains low amplitude spectra with an increase at frequencies above 15 kHz.

The intra- and inter-region variabilities are quantified by the distribution {P1, P2, P3, P4} of the spectra

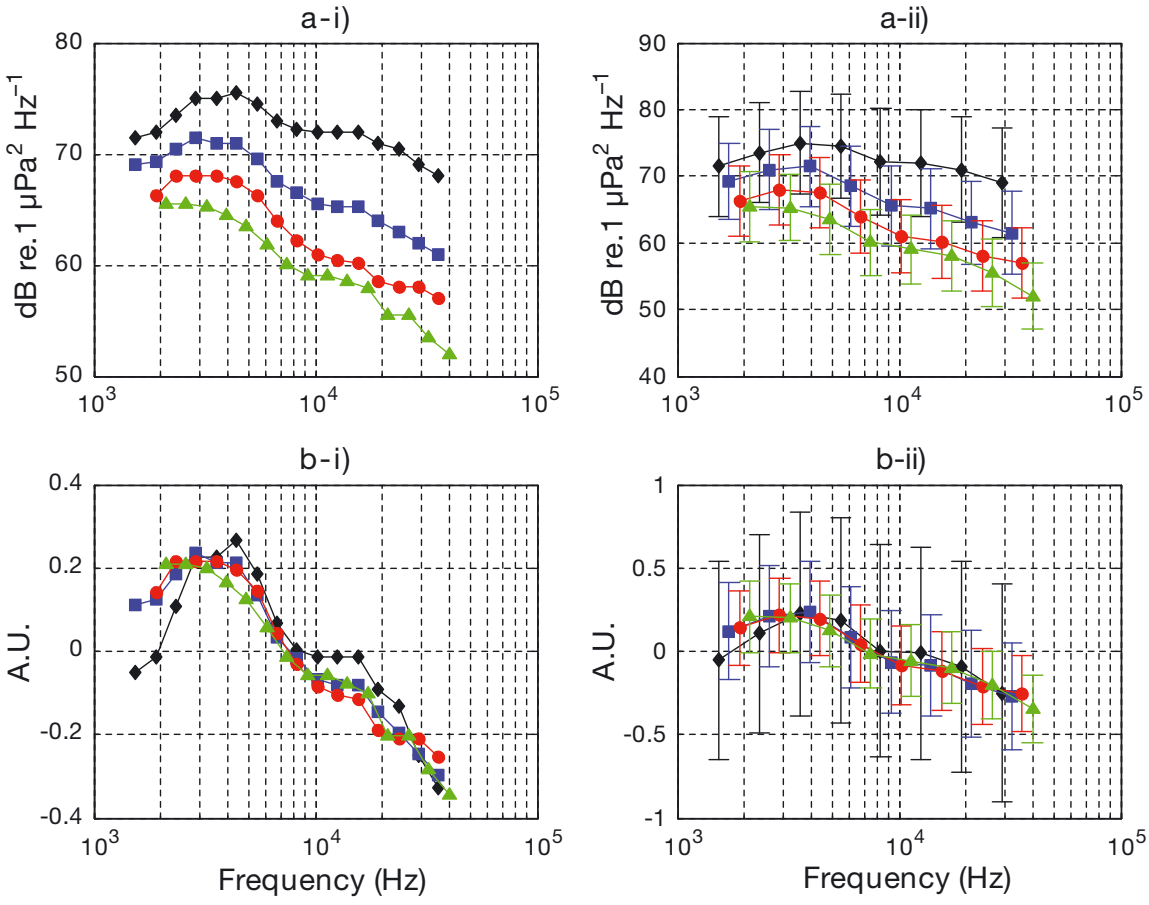

Fig. 6. Mean spectral shapes by region of descriptor *D*1 (a-i) without and (a-ii) with SD, and descriptor *D*2 (b-i) without and (b-ii) with SD. Black diamonds: Q1; blue squares: Q2; red circles: Q3; green triangles: Q4

of the snapshots of each region (Fig. 8). Regions Q1 to Q4 show significant differences in the combinations of the proportions of the spectral categories (Table 2), as shown by the results of the bootstrap MANOVA calculated on the proportions {P1, P2, P3} between all regions (Table 3). Proportions P1 and P2 decrease, while P4 increases with increasing distance to the coast (from Q1 to Q4, cf. Figs. 7c–f & 8).

Each proportion also differed between regions, as shown by the significant bootstrap ANOVA results (Table 3). Table 3 shows, for each proportion P1, P2, P3 and P4, the p-values of the ANOVA run on each couple of regions tested. This result implies that the benthic acoustic communities (Farina & James 2016) between the regions differ, and is greater between region Q1 and Q4.

Evaluation of the proportions {P1, P2, P3, P4} at the scale of a point of measurement (cf. Fig. 2) allows us to map these proportions over the regions Q1, Q2, Q3, Q4 and to compare these maps with that of SPL_{Imp} (cf. Fig. 9). The map of P1+P2 is similar to the map of SPL_{Imp}, with maximum values within the region Q1 close to the nearshore rocky reef, and a decrease from region Q1 to Q4. These 2 maps image the production of the loud impulses at the rocky reef and its propagation offshore. The higher values of P3 are more spread out over the entire study area, although some appear at the seagrass region. Contrary to P1+P2, P4 has its higher values offshore mainly above the coralligenous reefs.

DISCUSSION

The high-energy nature of benthic sound production in rocky reefs has regularly been underlined and described by the use of acoustic indices related to the signal's power (Radford et al. 2010, McWilliam & Hawkins 2013, Lillis et al. 2014b, Butler et al. 2016, Rossi et al. 2016a,b). It has been hypothesized that at small spatial scales (below a few km) these BIS (>2 kHz) produce a loud biophony that propagates

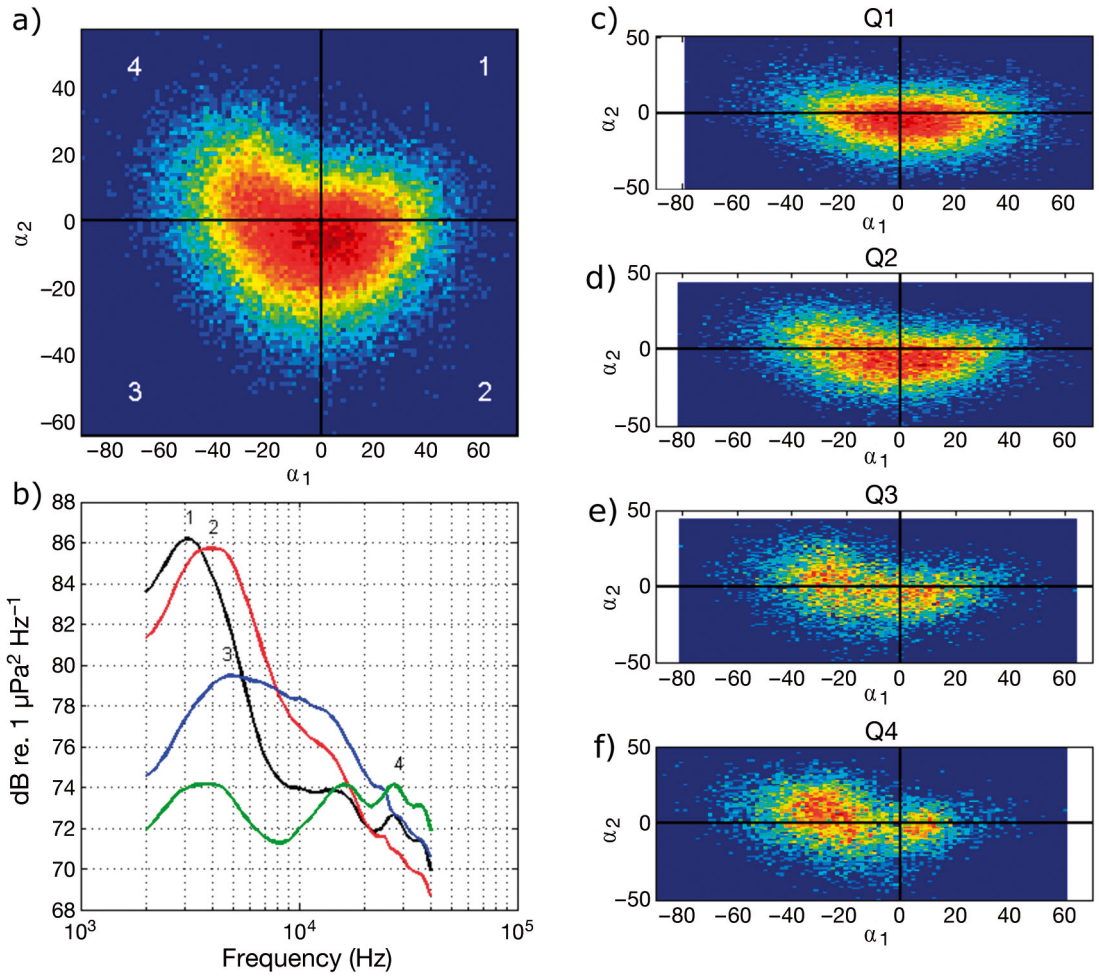

Fig. 7. (a) Probability density scores $\{\alpha_1, \alpha_2\}$ of the spectra of all measurement points. The numbers 1 to 4 identify the shape families (S1, S2, S3, S4). (b) Median spectrum for each category (black: S1; red: S2; blue: S3; green: S4). (c–f) Probability density scores $\{\alpha_1, \alpha_2\}$ for regions Q1 to Q4. Warm (cold) colors correspond to high (low) probabilities

offshore, invading and potentially masking low-power benthic emissions of other habitats (McWilliam & Hawkins 2013). Assuming that larvae have hearing abilities, the propagation distance of this high-energetic biophony defines the large distance of potential larval attraction from offshore to nearshore, but also degrades the spatial resolution of PAES in terms of biodiversity assessment through passive acoustics (Radford et al. 2011, McWilliam & Hawkins 2013, Piercy et al. 2014). Here, we estimated the propagation distances of rocky reef BIS, tested the hypothesis that it masks the biophony of other adjacent habitats, and proposed IDSS indices based on the diversity of the spectral shape that allows us to highlight and quantify differences in benthic sound productions, including low-power ones. We evaluated whether the use of IDSS improves the spatial resolution of the PAES at a sub-km scale (~200 m) compared to 'classical' acoustic indices based on sound pressure levels and power spectra.

Thanks to a regression on distance-based SPLs, the source level of the biophony of rocky reefs was estimated to be 147 dB re 1 µPa at 1 m. Lillis et al. (2014a) reported source levels ranging from 127 to 136 dB re 1 µPa at 1 m for a single oyster reef positioned within a large soft-bottom area. By extrapolating the source levels of coral reefs from the data reported in Piercy et al. (2014) (who used a parameterized geometrical spreading model as in the present study), source levels ranged from 120 to 144 dB re 1 µPa at 1 m, depending on the ecological status of the reef. The source level found in the present study is greater than but consistent with those reported elsewhere. This positive difference may be related to substrate type differences (rocky reef compared to oyster and coral reefs), animal densities, and the good environmental status of the bay of la Revellata. From the slope of the linear regression, TL was estimated to be -14 dB decade^{-1}. This value is intermediate between

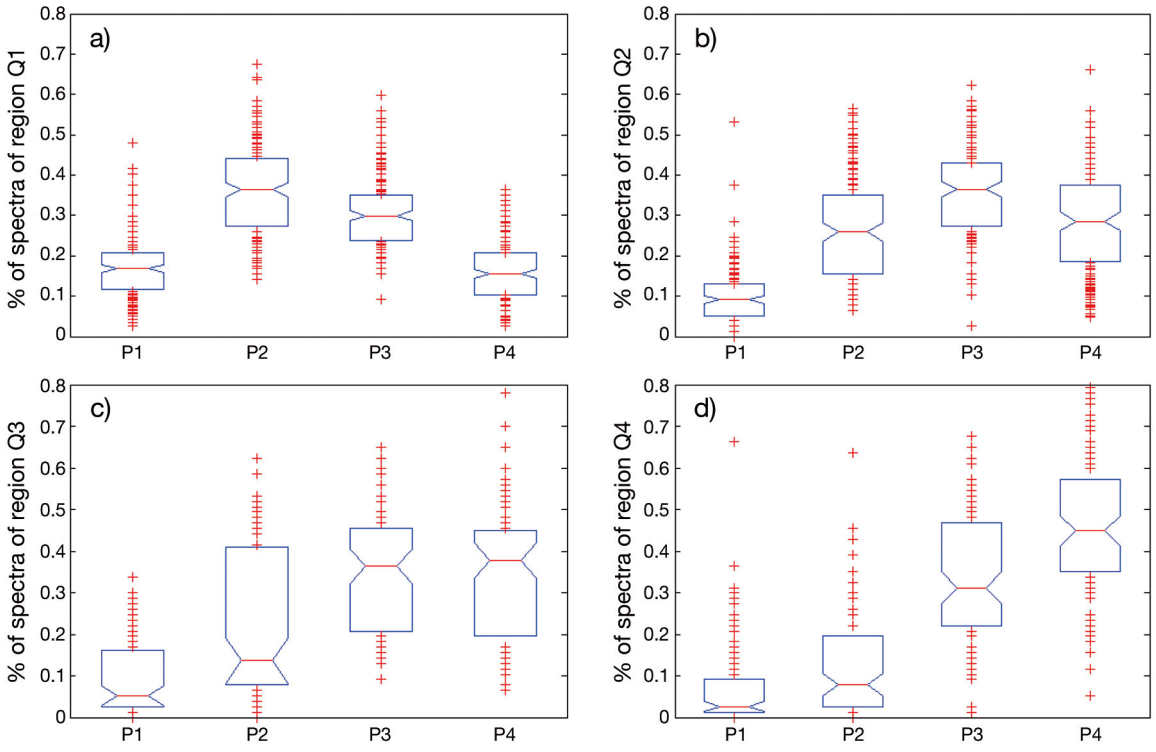

Fig. 8. Proportion {P1, P2, P3, P4} evaluated on 10 s snapshots for each region: (a) Q1, (b) Q2, (c) Q3 and (4) Q4. Boxplot limits — red bar: median (q_2); box: 25th (q_1) to 75th (q_3) percentiles; crosses: outliers; notch extremes: $q_2 \pm [1.57(q_3 - q_1)/\sqrt{(n)}]$, where n = no. of observations

spherical (−20 dB decade^{-1}) and cylindrical (−10 dB decade^{-1}) spreading losses. In the case of our study site, depth increases with distance to the coast, and the expected model is the spherical spreading loss model (Medwin & Clay 1997). This discrepancy (14 instead of 20 dB decade^{-1}) is likely a consequence of the so-called 'acoustic reef effect' (Radford et al. 2011). The rocky reef of the bay of la Revellata is not a punctual sound source, but rather produces a set of sounds that spread along 7 km of coast, thus creating an 'acoustic reef'. Radford et al. (2011) showed that this acoustic reef effect tends to compensate the TL, reducing the theoretical TL coefficient by a few dB. Compared to other studies that reported a TL of −8 dB decade^{-1} (Lillis et al. 2014a, Piercy et al. 2014), the TL coefficient found in this work is higher. In contrast to our study site, the bathymetry reported in the other study areas varied little and the theoretical model of expected TL was the cylindrical spreading loss model compensated by 2 to 3 dB of the acoustic reef effect rather than the spherical spreading loss model. Propagation distances of the biophony of the rocky reef of la Revellata ranged from 3680 m considering a wind speed of 3 m s^{-1} to 500 m with wind speeds attaining 12 m s^{-1}. These orders of magnitude are consistent with the findings reported by the scientific community. Lillis et al. (2014b) suggested that the propagation distance of the biophony of an oyster reef on a soft bottom habitat is greater than 500 m for sea states below 3 on Beaufort scale. Piercy et al. (2014) and Radford et al. (2011) reported propagation distances greater than 1500 m for coral and rocky reefs. The results presented here, based on the SPL_{Imp} descriptor, support the hypothesis that a strong biophony emanating from the rocky reef propagates offshore and invades other habitats within 500 to 3600 m depending on the wind regime. This also defines the spatial resolution of a PAES using SPL_{Imp} in terms of biodiversity assessment using passive acoustics: at a given position of measurement, the distant but loud impulses from the rocky reef propagate toward the hydrophone, are loud enough to mask the quieter impulses produced by benthic fauna adjacent to the hydrophone, and decrease the contrast on the map of acoustics indices.

By introducing the frequency dimension, soundscape description is richer and the spatial resolution may be enhanced. We tested whether any of the regions {Q1, Q2, Q3, Q4} produced a spectrum different than another region. The 4 regions, corresponding to different distances from the coast but also to different habitat types, differed significantly in terms

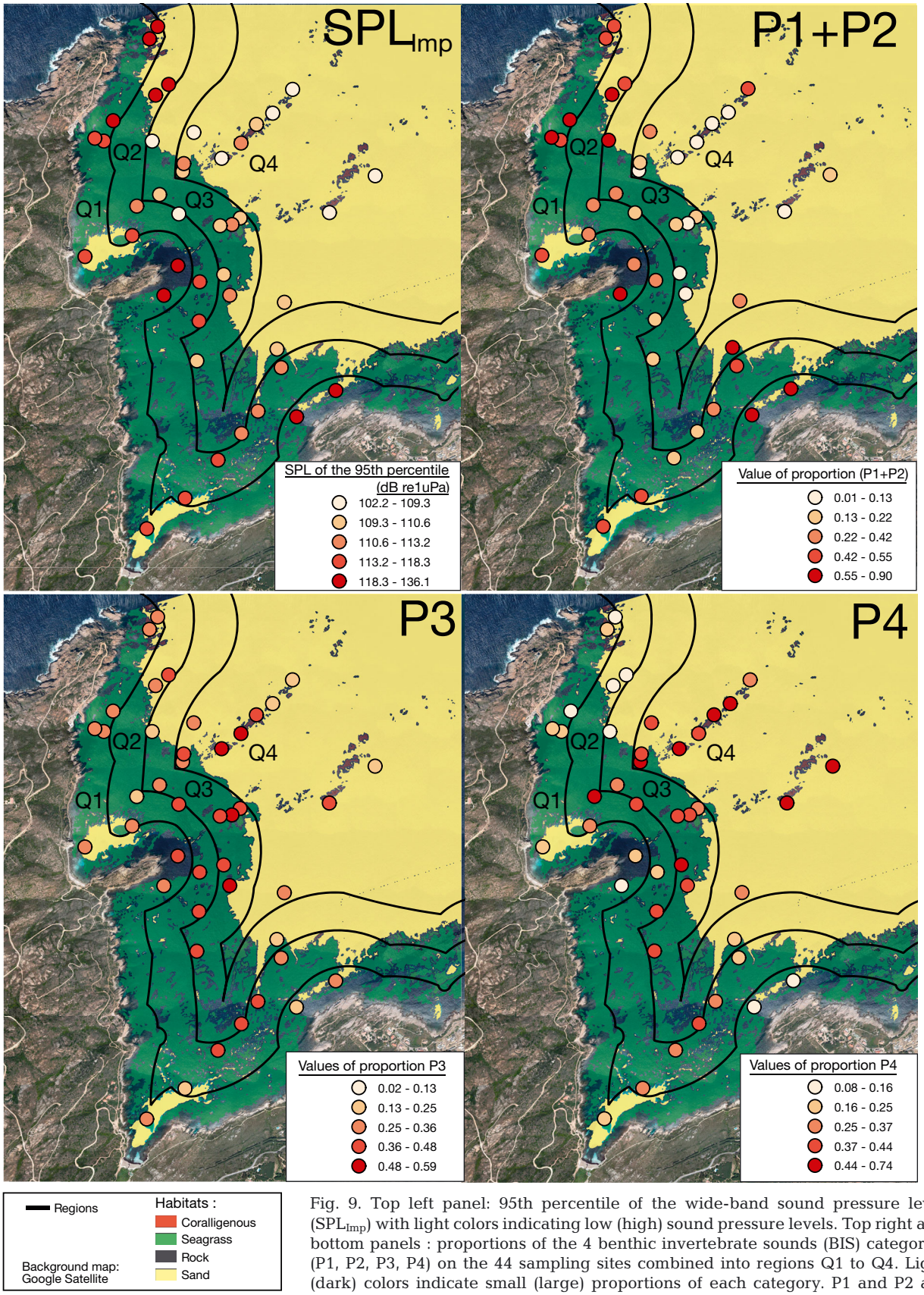

Fig. 9. Top left panel: 95th percentile of the wide-band sound pressure level (SPL_{lmp}) with light colors indicating low (high) sound pressure levels. Top right and bottom panels : proportions of the 4 benthic invertebrate sounds (BIS) categories (P1, P2, P3, P4) on the 44 sampling sites combined into regions Q1 to Q4. Light (dark) colors indicate small (large) proportions of each category. P1 and P2 are combined because their spectral shapes are similar (Fig. 7b)

Table 2. Proportions of the spectral families {P1, P2, P3, P4} contained in each region (Q1–Q4)

Region	Proportion				Total
	P1	P2	P3	P4	
Q1	0.19	0.37	0.30	0.14	1
Q2	0.12	0.28	0.32	0.28	1
Q3	0.10	0.21	0.31	0.38	1
Q4	0.12	0.18	0.28	0.42	1

Table 3. P1,P2,P3 Table: p-values of the bootstrap MANOVA run on each combination of 2 regions and for the 3 independent spectral families {P1, P2, P3} tested together. P1 Table, P2 Table, P3 Table and P4 Table: p-values of the bootstrap ANOVAs run on each combination of 2 regions and for each proportion of the spectral families {P1, P2, P3, P4}. *Italics* identify couples for which the hypothesis of an identical average cannot be rejected while **bold** indicates the couples for which this hypothesis can be rejected

		Q1	Q2	Q3	Q4
P1, P2, P3	Q1	*1*	**2.5×10^{-8}**	**1.1×10^{-11}**	**1.2×10^{-20}**
	Q2		*1*	**2.5×10^{-3}**	**3.9×10^{-8}**
	Q3			*1*	**1.1×10^{-3}**
	Q4				*1*
P1	Q1	*1*	**1.5×10^{-4}**	**2.5×10^{-4}**	**2.5×10^{-4}**
	Q2		*1*	*0.29*	*0.38*
	Q3			*1*	*0.66*
	Q4				*1*
P2	Q1	*1*	**1.2×10^{-4}**	**1.1×10^{-5}**	**2.5×10^{-12}**
	Q2		*1*	*0.18*	**3.5×10^{-5}**
	Q3			*1*	*0.07*
	Q4				*1*
P3	Q1	*1*	*0.50*	*0.39*	*0.25*
	Q2		*1*	*0.15*	*0.08*
	Q3			*1*	*0.52*
	Q4				*1*
P4	Q1	*1*	**1.9×10^{-8}**	**1.5×10^{-11}**	**1.3×10^{-19}**
	Q2		*1*	*0.06*	**2.5×10^{-7}**
	Q3			*1*	*0.05*
	Q4				*1*

of mean power spectra. This difference was only due to power differences and not the shape of the spectrum, with the amplitudes of the spectra decreasing from region Q1 to Q4 (Fig. 6a). In fact, no significant differences in shape were found after amplitude normalization of the spectra. Consequently, the 4 regions shared the same average spectral shapes (Fig. 6b). This finding is in line with that obtained by the SPL_{Imp} analysis. It is noteworthy that for region Q4 (distance to the nearest rocky reef: 514 to 1934 m), the spectra in the biogenic frequency band were still 20 dB above Wenz's model (for a wind speed of 3 m s^{-1}). Combined with the lack of spectral shape differences after amplitude normalization, our findings again support the hypothesis that a strong biophony emitted by the rocky reef propagates offshore, invading other habitats.

Adding the frequency dimension by comparing a single power spectrum is not sufficient to characterize areas with a small-scale mosaic of habitats because useful information about spectral diversity is not addressed. The here-proposed IDSS use of the first 2 components of the PCA based on normalized BIS spectra can depict this diversity and overcome the masking effect of loud 'acoustically invasive' sources such as snapping shrimps. The first 2 components of the PCA captured 55% of the total variance of the BIS. Given this strong descriptive power, the projection of the spectra on the first 2 eigenvectors of the PCA represents a good estimator of spectral shapes. In underwater acoustics, this approach has been used by Simard et al. (2016) to describe the variability of average spectra radiating from ships (74% of the variance explained) and to connect this variability to vessel characteristics (Simard et al. 2016). Kennedy et al. (2010) described the variability of the average spectra of biophony of coral reefs (73% of the variance captured) and linked them to their ecological characteristics. We enhanced the approach proposed in these 2 studies, accounting for the diversity of spectral shapes by working on the 76 highest spectra (highest 5% of spectra which are the nearest benthic pulses) contained in a 10 s segment. The distribution of the first 2 coordinates of the PCA of the normalized spectrums (cf. Fig. 7a) is continuous and does not present well-separated modes that may indicate and define obvious acoustics families. By inspecting this distribution as a function of the region Q1, Q2, Q3, Q4 (cf. Fig. 7c–f), the proportions of the first 2 coordinates $\{\alpha_1, \alpha_2\}$ of the PCA in the 4 quarters (P1: $\alpha_1 > 0$, $\alpha_2 > 0$; P2: $\alpha_1 > 0$, $\alpha_2 < 0$; P3: $\alpha_1 < 0$, $\alpha_2 < 0$; P4: $\alpha_1 < 0$, $\alpha_2 > 0$) clearly change with the index i of the region Q_i. The 4 mean spectral shapes (Fig. 7b) of each of the 4 quarters have ecological relevance since they are similar to ones associated with benthic species (Au et Banks 1998, Radford et al. 2008, Coquereau et al. 2016a,b). Relying on these 2 ascertainments, we propose to split the spectral shapes into 4 families, 1 for each of the 4 quarters. These 4 families of spectral shapes can describe the acoustic diversity of a mosaic of habitats and can serve to attempt a quantification of the invasive nature of the rocky reef's BIB of the bay of la Revellata. Overall, 12% of the BIS belong to category S1 with a marked maximum around 3 kHz and a 2 kHz

bandwidth; 29% belong to the category S2, with a marked maximum around 4 kHz, an increase around 10 kHz and a 2 kHz bandwidth; 33% belong to the spectral shape category S3, characterized by broadband pulses [8–20 kHz]; and 26% of all BIS spectra belong to category S4, defined by a spectral increase at frequencies above 15 kHz. Families S1 and S2 are similar, consist of high-energy spectra and together represent 41% of the BIS. Category S3 contains intermediate amplitude spectra and category S4, low-power spectra. Regions Q1 to Q4 shared the same acoustics dictionary because each hosted members of the families S1 to S4, but they showed significant differences in the proportions of these spectral families (Fig. 8). Families S1 and S2 dominate the biophony of region Q1 (56% of all BIS). The proportion of BIS belonging to these 2 families decreased with increasing distance to the coast: 50% of the BIS of region Q2, 31% of region Q3 and 30% of region Q4. This variability of the proportions of S1 and S2 depending on the distance to the coast suggests that the rocky reef produces low frequency, high-energetic transient sounds that propagate offshore. This pattern is consistent with the results of the power-based descriptors. In addition, the IDSS of S1 and S2 allow us to quantify these dominant rocky benthic sound sources (Fig. 9). Category S3 was uniformly distributed across regions (30 ± 1%), while the proportion of category S4 increased from Q1 to Q4, from 14 to 42%. In contrast to regions Q1 and Q2, Q4 is dominated by low-energy, high-frequency BIS. This result probably best emphasizes the power of the descriptor proposed here in depicting soundscape differences despite the presence of a loud masking sound source. These findings also show that the introduction of the diversity of spectral shapes of BIS allows refining the characterization of the structure of the soundscape in the bay of la Revellata. The spectral shape descriptors are mapped, allowing us to link acoustic information to other habitats or ecological features (Fig. 9). In fact, the proportions of the different acoustics families can also reveal habitat-specific features or signatures. Coralligenous reefs largely characterize region Q4, and the predominant presence of high-frequency sounds of category S4 suggests the presence of a specific coralligenous reef fauna. Currently, for our database, it is premature to associate each spectral category or their proportions to assemblages of benthic species or their behaviors. Nevertheless, families S1 and S2 are compatible with sounds emitted by snapping shrimp (Knowlton & Moulton 1963, Au & Banks 1998) and feeding sea urchins (Radford et al. 2008). However, Coquereau et al. (2016a) also showed that spectral characteristics (peak frequency, bandwidth, level) show wide variations within and between species of the same category. The nutrition of common sea urchins *Echinus esculentus*, for instance, produces peak frequencies ranging from 9 to 60 kHz and the peak frequencies of snapping shrimp snaps *Athanas nitescens* have 2 modes, with peaks at 9 and at 33 kHz. Although additional effort is needed to link spectral shapes to benthic communities or species, the 4 families reported here represent acoustic benthic communities and their diversities. Their proportions describe the richness at each sampling point. The sources of the spectral families could be identified using tank-based experiments (Di Iorio et al. 2012, Coquereau 2016a) or semi-natural *in situ* enclosures (Watanabe et al. 2002, Radford et al. 2008). When a 'dictionary of BIS' is established, then the diversity of the benthic biophony will provide information on the diversity of the soniferous species *in situ*.

It remains to be investigated whether (1) IDSS provides similar results in other areas with different or similar small-scale habitat mosaics, as for instance the one described by McWilliam & Hawkins (2013) in the North Atlantic; and (2) the eigenvector database from the PCA for a given site could be used to describe the diversity of spectral forms at other sites.

The diversity of spectral shapes provides new and more explanatory information to that extracted from 'classically used' power descriptors or BIS counts. It enriches our understanding of the spatial structure of a soundscape by providing access to less powerful phenomena despite the presence of a high-energy sound source. Furthermore, our results show that the use of PCA eigenvalues to describe spectral shapes can be used to quantify their diversity and thus the diversity of the benthic acoustic community of a site. In this work, characterizing the diversity of spectral shapes allowed us to reduce the spatial resolution to about 200 m, a more relevant ecological scale for the study of benthic communities (Archambault & Bourget 1996).

This may also have implications for larval recruitment, as diversity of spectral shapes can provide an additional cue. Power-based acoustic features appear to play a role in the detection of suitable habitats at long distances during the passage of a larvae from the pelagic to the coastal phase of development (Tolimieri et al. 2000, Montgomery et al. 2006, Stanley et al. 2012, Eggleston et al. 2016). To our knowledge, it is unknown whether larvae are capable of perceiving spectral shape diversity or are able to use this information as an additional cue for habitat

selection at smaller distances. Finally, the here-proposed descriptor shows promise for use in habitat quality/degradation assessment, and more generally PAES of vulnerable marine areas.

Acknowledgements. C.G. and L.D.I. were supported by a grant of the chair of researches CHORUS of the Grenoble Institute of Technology Foundation. This work is part of the SEAcoustics 2014 project cofounded by the French Water Agency Rhone Mediterranean Corsica (AE RMC). We thank STARESO for sharing their valuable knowledge of the area through the research program STARE-CAPMED. We thank Sabiod and GDR MADICS (Professor H. Glotin) for partial financial support of the purchase of the acoustics instrumentation; STARESO for the partial financial support of *in situ* measurements; and Lucas Bérenger and Julie Castera (Télédetection Biologie Marine Environnement) for their help during the 2014 Revellata campaign. J.L. was supported by a PhD grant from France Energies Marines (FEM) and French '*Région Bretagne*' within the research program 'Benthoscope' of FEM.

LITERATURE CITED

Acevedo-Gutiérrez A, Stienessen SC (2004) Bottlenose dolphins (*Tursiops truncatus*) increase number of whistles when feeding. Aquat Mamm 30:357–362

Amorim MCP (2006) Diversity of sound production in fish. In: Ladich F, Collin SP, Moller P, Kapoor BG (eds) Communication in fishes, Vol 1. Science Publishers, Endfield, NH, p 71–104

Anderson MJ, Millar RB (2004) Spatial variation and effects of habitat on temperate reef fish assemblages in northeastern New Zealand. J Exp Mar Biol Ecol 305:191–221

Archambault P, Bourget E (1996) Scales of coastal heterogeneity and benthic intertidal species richness, diversity and abundance. Mar Ecol Prog Ser 136:111–121

Archambault P, Bourget E (1999) Influence of shoreline configuration on spatial variation of meroplanktonic larvae, recruitment and diversity of benthic subtidal communities. J Exp Mar Biol Ecol 238:161–184

Au WW, Banks K (1998) The acoustics of the snapping shrimp *Synalpheus parneomeris* in Kaneohe Bay. J Acoust Soc Am 103:41–47

Au WW, Hastings MC (2008) Principles of marine bioacoustics. Springer, New York, NY

Bell JD, Westoby M (1986) Variation in seagrass height and density over a wide spatial scale: effects on common fish and decapods. J Exp Mar Biol Ecol 104:275–295

Bertucci F, Parmentier E, Berten L, Brooker RM, Lecchini D (2015) Temporal and spatial comparisons of underwater sound signatures of different reef habitats in Moorea Island, French Polynesia. PLOS ONE 10:e0135733

Buscaino G, Ceraulo M, Pieretti N, Corrias V and others (2016) Temporal patterns in the soundscape of the shallow waters of a Mediterranean marine protected area. Sci Rep 6:34230

Butler J, Stanley JA, Butler MJ IV (2016) Underwater soundscapes in near-shore tropical habitats and the effects of environmental degradation and habitat restoration. J Exp Mar Biol Ecol 479:89–96

Chitre M, Legg M, Koay TB (2012) Snapping shrimp dominated natural soundscape in Singapore waters. Contrib Mar Sci 2012:127–134

Coquereau L, Grall J, Chauvaud L, Gervaise C, Clavier J, Jolivet A, Di Iorio L (2016a) Sound production and associated behaviours of benthic invertebrates from a coastal habitat in the north-east Atlantic. Mar Biol 163:1–13

Coquereau L, Grall J, Clavier J, Jolivet A, Chauvaud L (2016b) Acoustic behaviours of large crustaceans in NE Atlantic coastal habitats. Aquat Biol 25:151–163

Coquereau L, Jolivet A, Hégaret H, Chauvaud L (2016c) Short-term behavioural responses of the great scallop *Pecten maximus* exposed to the toxic alga *Alexandrium minutum* measured by accelerometry and passive acoustics. PLOS ONE 11:e0160935

Coquereau L, Lossent J, Grall J, Chauvaud L (2017) Marine soundscape shaped by fishing activity. R Soc Open Sci 4: 160606

Crawford JD, Jacob P, Benech V (1997) Sound production and reproductive ecology of strongly acoustic fish in Africa: *Pollimyrus isidori*, Mormyridae. Behaviour 134: 677–725

Di Iorio L, Gervaise C, Jaud V, Robson AA, Chauvaud L (2012) Hydrophone detects cracking sounds: non-intrusive monitoring of bivalve movement. J Exp Mar Biol Ecol 432-432:9–16

Efron B, Tibshirani R (1985) The bootstrap method for assessing statistical accuracy. Behaviormetrika 12:1–35

Eggleston DB, Lillis A, Bohnenstiehl DR (2016) Soundscapes and larval settlement: larval bivalve responses to habitat-associated underwater sounds. In: Popper AN, Hawkins A (eds) The effects of noise on aquatic life II. Springer, New York, NY, p 255–263

Ellers O (1995) Discrimination among wave-generated sounds by a swash-riding clam. Biol Bull (Woods Hole) 189:128–137

Farina A, James P (2016) The acoustic communities: definition, description and ecological role. Biosystems 147: 11–20

Ferguson BG, Cleary JL (2001) *In situ* source level and source position estimates of biological transient signals produced by snapping shrimp in an underwater environment. J Acoust Soc Am 109:3031–3037

Gervaise C, Simard Y, Roy N, Kinda B, Ménard N (2012) Shipping noise in whale habitat: characteristics, sources, budget, and impact on belugas in Saguenay–St. Lawrence Marine Park hub. J Acoust Soc Am 132:76–89

Glass GV, Peckham PD, Sanders JR (1972) Consequences of failure to meet assumptions underlying the fixed effects analyses of variance and covariance. Rev Edu Res 42: 237–288

Gobert S, Sartoretto S, Rico-Raimondino V, Andral B, Chery A, Lejeune P, Boissery P (2009) Assessment of the ecological status of Mediterranean French coastal waters as required by the Water Framework Directive using the *Posidonia oceanica* Rapid Easy Index: PREI. Mar Pollut Bull 58:1727–1733

Gobert S, Chéry A, Volpon A, Pelaprat C, Lejeune P (2014) The seascape as an indicator of environmental interest and quality of the Mediterranean benthos: the *in situ* development of a description index: the LIMA. In: Musard O, Le Dû-Blayo L, Francour P, Beurier JP, Feunteun E, Talassinos L (eds) Underwater seascapes. Springer, New York, NY, p 277–291

Harris SA, Shears NT, Radford CA (2016) Ecoacoustic indices as proxies for biodiversity on temperate reefs. Methods Ecol Evol 7:713–724

Hastings PA, Širović A (2015) Soundscapes offer unique opportunities for studies of fish communities. Proc Natl Acad Sci USA 112:5866–5867

Hawkins AD (1986) Underwater sound and fish behaviour. In: Pitcher TJ (ed) The behaviour of teleost fishes. Springer, Boston, MA, p 114–151

Hildebrand JA (2009) Anthropogenic and natural sources of ambient noise in the ocean. Mar Ecol Prog Ser 395:5–20

Holon F, Boissery P, Guilbert A, Freschet E, Deter J (2015) The impact of 85 years of coastal development on shallow seagrass beds (*Posidonia oceanica* L. (Delile)) in south eastern France: a slow but steady loss without recovery. Estuar Coast Shelf Sci 165:204–212

Huijbers CM, Nagelkerken I, Lössbroek PAC, Schulten IE, Siegenthaler A, Holderied MW, Simpson SD (2012) A test of the senses: fish select novel habitats by responding to multiple cues. Ecology 93:46–55

Johnson MW, Everest FA, Young RW (1947) The role of snapping shrimp (*Crangon* and *Synalpheus*) in the production of underwater noise in the sea. Biol Bull (Woods Hole) 93:122–138

Kennedy E, Holderied M, Mair J, Guzman H, Simpson S (2010) Spatial patterns in reef-generated noise relate to habitats and communities: evidence from a Panamanian case study. J Exp Mar Biol Ecol 395:85–92

Kinda GB, Simard Y, Gervaise C, Mars JI, Fortier L (2013) Under-ice ambient noise in eastern Beaufort Sea, Canadian Arctic, and its relation to environmental forcing. J Acoust Soc Am 134:77–87

Kinda GB, Simard Y, Gervaise C, Mars JI, Fortier L (2015) Arctic underwater noise transients from sea ice deformation: characteristics, annual time series, and forcing in Beaufort Sea. J Acoust Soc Am 138:2034–2045

Knowlton RE, Moulton JM (1963) Sound production in the snapping shrimps *Alpheus* (*Crangon*) and *Synalpheus*. Biol Bull (Woods Hole) 125:311–331

Krause B (1987) Bioacoustics: habitat ambience & ecological balance. Whole Earth Rev 57:14–16

Lejeune P, Abadie A, Binard M, Biondo R, Borges A (2013) STARE-CAPMED (STation of Reference and rEsearch on Change of local and global Anthropogenic Pressures on Mediterranean Ecosystems Drifts): rapport d'activité 2013. STARESO, Calvi

Lillis A, Eggleston DB, Bohnenstiehl DR (2014a) Estuarine soundscapes: distinct acoustic characteristics of oyster reefs compared to soft-bottom habitats. Mar Ecol Prog Ser 505:1–17

Lillis A, Eggleston DB, Bohnenstiehl DR (2014b) Soundscape variation from a larval perspective: the case for habitat-associated sound as a settlement cue for weakly swimming estuarine larvae. Mar Ecol Prog Ser 509:57–70

Lillis A, Bohnenstiehl DR, Eggleston DB (2015) Soundscape manipulation enhances larval recruitment of a reef-building mollusk. PeerJ 3:e999

Luczkovich JJ, Mann DA, Rountree RA (2008) Passive acoustics as a tool in fisheries science. Trans Am Fish Soc 137:533–541

Mann DA, Grothues TM (2009) Short-term upwelling events modulate fish sound production at a mid-Atlantic Ocean observatory. Mar Ecol Prog Ser 375:65–71

Mathias D, Gervaise C, Di Iorio L (2016) Wind dependence of ambient noise in a biologically rich coastal area. J Acoust Soc Am 139:839–850

McWilliam JN, Hawkins AD (2013) A comparison of inshore marine soundscapes. J Exp Mar Biol Ecol 446:166–176

Medwin H, Clay CS (1997) Fundamentals of acoustical oceanography. Academic Press, San Diego, CA

Montgomery JC, Jeffs A, Simpson SD, Meekan M, Tindle C (2006) Sound as an orientation cue for the pelagic larvae of reef fishes and decapod crustaceans. Adv Mar Biol 51: 143–196

Nedelec SL, Simpson SD, Holderied M, Radford AN, Lecellier G, Radford C, Lecchini D (2015) Soundscapes and living communities in coral reefs: temporal and spatial variation. Mar Ecol Prog Ser 524:125–135

Parmentier E, Berten L, Rigo P, Aubrun F, Nedelec SL, Simpson SD, Lecchini D (2015) The influence of various reef sounds on coral-fish larvae behaviour. J Fish Biol 86: 1507–1518

Patek SN (2001) Spiny lobsters stick and slip to make sound. Nature 411:153–154

Piercy JJB, Codling EA, Hill AJ, Smith DJ, Simpson SD (2014) Habitat quality affects sound production and likely distance of detection on coral reefs. Mar Ecol Prog Ser 516:35–47

Pijanowski BC, Villanueva-Rivera LJ, Dumyahn SL, Farina A and others (2011) Soundscape ecology: the science of sound in the landscape. Bioscience 61:203–216

Popper AN, Salmon M, Horch KW (2001) Acoustic detection and communication by decapod crustaceans. J Comp Physiol A 187:83–89

QGIS Development Team (2009) Quantum GIS Geographic Information System. Open Source Geospatial Foundation. http://qgis.osgeo.org

Radford CA, Jeffs A, Tindle CT, Montgomery JC (2008) Resonating sea urchin skeletons create coastal choruses. Mar Ecol Prog Ser 362:37–43

Radford CA, Stanley JA, Tindle CT, Montgomery JC, Jeffs AG (2010) Localised coastal habitats have distinct underwater sound signatures. Mar Ecol Prog Ser 401:21–29

Radford CA, Tindle CT, Montgomery JC, Jeffs AG (2011) Modelling a reef as an extended sound source increases the predicted range at which reef noise may be heard by fish larvae. Mar Ecol Prog Ser 438:167–174

Richir J, Abadie A, Binard M, Biondo R and others (2014) STARE-CAPMED (STAtion of Reference and rEsearch on Change of local and global Anthropogenic Pressures on Mediterranean Ecosystems Drifts). STARESO, Calvi

Rossi T, Nagelkerken I, Pistevos JCA, Connell SD (2016a) Lost at sea: ocean acidification undermines larval fish orientation via altered hearing and marine soundscape modification. Biol Lett 12:20150937

Rossi T, Connell SD, Nagelkerken I (2016b) Silent oceans: ocean acidification impoverishes natural soundscapes by altering sound production of the world's noisiest marine invertebrate. Proc R Soc B 283:20153046

Rountree RA, Gilmore RG, Goudey CA, Hawkins AD, Luczkovich JJ, Mann DA (2006) Listening to fish. Fisheries (Bethesda, MD) 31:433–446

Ruppé L, Clément G, Herrel A, Ballesta L, Décamps T, Kéver L, Parmentier E (2015) Environmental constraints drive the partitioning of the soundscape in fishes. Proc Natl Acad Sci USA 112:6092–6097

Seytre C, Francour P (2009) The Cap Roux MPA (Saint-Raphaël, French Mediterranean): changes in fish assemblages within four years of protection. ICES J Mar Sci 66: 180–187

Simard Y, Roy N, Gervaise C, Giard S (2016) Analysis and

modeling of 255 source levels of merchant ships from an acoustic observatory along St. Lawrence Seaway. J Acoust Soc Am 140:2002–2018

Simpson SD, Meekan M, Montgomery J, McCauley R, Jeffs A (2005) Homeward sound. Science 308:221

Stanley JA, Radford CA, Jeffs AG (2012) Location, location, location: finding a suitable home among the noise. Proc R Soc B 279:3622–3631

Sueur J, Farina A (2015) Ecoacoustics: the ecological investigation and interpretation of environmental sound. Biosemiotics 8:493–502

Sueur J, Pavoine S, Hamerlynck O, Duvail S (2008) Rapid acoustic survey for biodiversity appraisal. PLOS ONE 3: e4065

Sueur J, Farina A, Gasc A, Pieretti N, Pavoine S (2014) Acoustic indices for biodiversity assessment and landscape investigation. Acta Acust United Acust 100: 772–781

Terlizzi A, Anderson MJ, Fraschetti S, Benedetti-Cecchi L (2007) Scales of spatial variation in Mediterranean subtidal sessile assemblages at different depths. Mar Ecol Prog Ser 332:25–39

Tolimieri N, Jeffs AG, Montgomery JC (2000) Ambient sound as a cue for navigation by the pelagic larvae of reef fishes. Mar Ecol Prog Ser 207:219–224

Urick RJ (1967) Principles of underwater sound for engineers. McGraw-Hill, New York, NY

Versluis M, Schmitz B, von der Heydt A, Lohse D (2000) How snapping shrimp snap: through cavitating bubbles. Science 289:2114–2117

Watanabe M, Sekine M, Hamada E, Ukita M, Imai T (2002) Monitoring of shallow sea environment by using snapping shrimps. Water Sci Technol 46:419–424

Wenz GM (1962) Acoustic ambient noise in the ocean: spectra and sources. J Acoust Soc Am 34:1936–1956

Zenil HP, Encomio VG, Gilmore RG (2011) Passive acoustics as a monitoring tool for evaluating oyster reef restoration. J Acoust Soc Am 129:2698

Editorial responsibility: Claire Paris, Miami, Florida, USA

Submitted: April 4, 2017; Accepted: October 16, 2017
Proofs received from author(s): December 18, 2017